

Ghrelin suppresses hypoxia/reoxygenation-induced H9C2 cell pyroptosis via NLRP3

Li Xu¹, Jie Su², Caili Du³, Hui Liu⁴, Wei Lv^{5*}¹Department of Cardiology Intensive Care, Central Hospital Affiliated to ShanDong First Medical University, Jinan 250013, China²Department of Infectious Diseases, Central Hospital Affiliated to Shangdong First Medical University, Jinan 250013, China³Department of Nuclear Medicine, Jinan Central Hospital, Jinan 250013, China⁴Department of Thyroid Surgery, Jinan Central Hospital, Jinan 250013, China⁵Department of Cardiovascular Unit 2, Jinan Central Hospital, Jinan 250013, China

ARTICLE INFO

Original paper

Article history:

Received: June 17, 2023

Accepted: November 10, 2023

Published: December 10, 2023

Keywords:

Ghrelin, NLRP3, caspase-1, H/R, cell pyroptosis

ABSTRACT

To study the influence of ghrelin on hypoxia/reoxygenation (H/R) induced H9C2 cell pyroptosis by regulating NLRP3, H9C2 cells were categorized into 3 distinct groups: the control group (referred to as Control), the hypoxia-exposed group (abbreviated as H), and the hypoxia/reoxygenation-exposed group (referred to as H/R). The expression of ghrelin and NLRP3 was determined. Ghrelin overexpression cell line was established to analyze its effects on cell viability, cell cycle and apoptosis. Simultaneously, the assessment of NLRP3 and Caspase-1 expression levels was conducted. To further inspect the effect of ghrelin on H/R treated H9C2 cells via NLRP3, the experimental setups were formulated as follows: control group (Control), H/R group (abbreviated as H/R), Ghrelin overexpression group (Ghrelin), ghrelin overexpression and NLRP3 overexpression group (Ghrelin + NLRP3), NLRP3 overexpression group (NLRP3), NLRP3 negative control group (NLRP3-NC). The experiments mentioned above were performed in each group. In comparison to control, H/R cells expressed significantly lower levels of ghrelin, but higher levels of NLRP3. Further, a noteworthy reduction in cell viability was evident within the H/R group, with much more cells in the G0/G1 phase and less in the S phase, and with elevated cell death rate and protein levels of NLRP3 and caspase-1 ($P < 0.05$). Overexpression of ghrelin was capable of increasing cell viability, reducing G0/G1 cell number while increasing S phase cells. Ghrelin overexpression could suppress cell apoptosis and both NLRP3 and caspase-1 expressions. NLRP3 overexpression could diminish the beneficial impacts of ghrelin on H/R-treated H9C2 cells. Ghrelin exhibited the capability to suppress H/R-induced H9C2 cell pyroptosis through inhibition of NLRP3.

Doi: <http://dx.doi.org/10.14715/cmb/2023.69.13.30>Copyright: © 2023 by the C.M.B. Association. All rights reserved. 

Introduction

Myocardial ischemia-reperfusion is commonly observed in the clinic, which might cause oxidative stress and tissue damage in the heart (1, 2). Various hypoxia/reoxygenation (H/R) models have been established to mimic myocardial ischemia-reperfusion, among which rat cardiomyoblast cell line H9C2 was widely adopted by researchers to investigate H/R-induced injuries (3-5). Several studies focused on the mechanisms that regulated cell death of H/R treated H9C2 cells, including sonic hedgehog signaling and Akt/mTOR pathway (6, 7).

Pyroptosis is a gasdermin D-mediated programmed necrotic cell death initiated by NACHT, LRR, and PYD domains-containing protein 3 (NLRP3) inflammasome (8, 9). The formation of NLRP3 inflammasome could be triggered by diverse stress conditions such as pathogen invasion and oxidative stress, resulting in the activation of caspase-1 which is capable of cleaving gasdermin D to promote pore formation on the cell membrane (8-10). The role of pyroptosis in cardiovascular diseases has been intensively studied in the past decade to find endogenous modulators and develop new therapies for the disease (11, 12). Oxidative stress-induced NLRP3-caspase-1 axis activation might lead to cell pyroptosis thus causing myocar-

dial infarction (13, 14).

Ghrelin, identified as the endogenous ligand for the growth hormone secretagogue receptor, was initially isolated from the stomach of rats in 1999 (15). Ghrelin has been documented to exert its effects in various systems including the cardiovascular, gastrointestinal, and immune systems. In cardiovascular diseases, ghrelin inhibited ischemia-induced cardiac remodeling and arrhythmias (16, 17). Former researches have indicated that ghrelin can inhibit cardiac cell apoptosis in the context of cardiac remodeling following the induction of myocardial infarction through experimental means in rats. This inhibition is achieved through the activation of the Raf-MEK1/2-ERK1/2 pathway (18). Additionally, ghrelin has been associated with the NLRP3 inflammasome pathway and pyroptosis, which inhibited the NLRP3 inflammasome pathway to alleviate neuroinflammation and disease progression (19). Moreover, Wang et al found that ghrelin could protect the heart against ischemia reperfusion-induced injury through inhibiting oxidative stress and inflammation, which might be associated with the NLRP3 pathway (20). However, the pyroptosis-connected mechanisms of ghrelin remained largely unclear in ischemia-reperfusion-induced myocardial infarction.

Here, the study compared the differences in ghrelin

* Corresponding author. Email: lvwei202012@126.com

expression between hypoxia and hypoxia/reoxygenation in H9C2 cells and further demonstrated that ghrelin possessed the capability to suppress H/R-induced H9C2 cell pyroptosis via NLRP3-caspase-1 axis. This finding suggested a potential protective effect of ghrelin in myocardia, which might provide a new option to treat ischemia-reperfusion-induced myocardial infarction.

Materials and Methods

Cell culture and grouping

We purchased the H9C2 cells from BeNa Culture Collection (BNCC295075), Beijing, and cultured them in DMEM (Hyclone, South Logan, UT, USA) + 10% fetal bovine serum + 1% penicillin/streptomycin medium in 37°C incubator containing 5% CO₂.

The H9C2 cells were categorized into three distinct groups based on varied treatment protocols: control group (Control): cells were not treated at all; hypoxia group (H): cells were treated with 5 h oxygen deprivation; H/R group (H/R): cells were treated with 5 h oxygen deprivation followed with 1 h reoxygenation. The H/R cell model was established as mentioned previously: 5 h oxygen deprivation (1% O₂, 94% N₂, 5% CO₂) and 1 h reoxygenation (5% CO₂) (21).

Cell transfection

Cells were digested with 0.25% trypsin and subcultured in 6-well plates. Cell transfections were conducted at cell confluency 30-50%. Ghrelin sequence and NLRP3 sequence were constructed into pcDNA3.1, respectively. The target plasmids were transfected using the Lipofectamine 2000 kit. The target plasmids were purchased from Genechem (Shanghai Genechem Co., Ltd, Shanghai, China). Cells were transfected for 72 h to continue the study.

Cell groups

We divided the H9C2 cells into several groups: (1) control group (Control): cells were cultured as normal; (2) H/R group (H/R): cells were not transfected, but treated with 5 h oxygen deprivation followed with 1 h reoxygenation; (3) Ghrelin overexpression negative control group (NC): cells underwent transfection with 4 µg pcDNA-empty plasmid for 72 h before H/R, (4) Ghrelin overexpression group (Ghrelin): cells underwent transfection with 4 µg pcDNA-ghrelin plasmid (5'-TGCTCTAGAA-TGCCCTCCCCAGGGACCGTCT-3') for 72 h before H/R (22).

To further investigate the role of NLRP3 in the process, cells were grouped as below: (1) control group (Control), (2) H/R group (H/R), (3) Ghrelin overexpression group (Ghrelin), (4) Ghrelin overexpression with NLRP3 overexpression group (Ghrelin+NLRP3): cells were transfected with pcDNA-ghrelin plasmids and pc-NLRP3 plasmids for 72 h before H/R (23), (5) NLRP3 overexpression group (NLRP3): cells were transfected with 4 µg pcDNA-NLRP3 plasmids for 72 h before H/R, (6) NLRP3 negative control group (NLRP3-NC), cells were transfected with 4 µg pcDNA-empty plasmid for 72 h before H/R.

RT-PCR

Cells of each group were collected and the total RNA of each group was extracted with TRIzol kit (15596-018,

Life Technology, Gaithersburg, MD, USA) according to the instructor after establishing the H/R cell model. The concentration of RNA extracted was determined and then RNA was subjected to reverse transcription using a reverse transcription kit (Qiagen, Duesseldorf, Germany). Mastercycler nexus (Light Cycler96, Roche, Basel, Switzerland) was adopted for qRT-PCR to obtain the cycle number of each sample at the threshold. The qRT-PCR program was set as: The initial denaturation was carried out at 94°C for 3 minutes; denaturation was conducted at 94°C for 30 s, primer annealing at 60°C for 30 s, elongation at 72°C for 20 s, cycled for 40 times. RNA quantification was achieved by the 2^{-ΔΔCT} method. Primer sequences were listed below: Ghrelin, Forward: 5'-GGTGTCTTCAGCGACTATC-TGC-3'; Reverse: 5'-TCCTCCTCTGCCTCTTCTGC-3'; NLRP3, Forward: 5'-TCTGTTTCATTGGCTGCGGA-3', Reverse: 5'-GCCTTTTTTCGAAGTTGCCGT-3'; β-actin, Forward: 5'-GTCACCAACTGGGACGATA-3', Reverse: 5'-GGGGTGTTGAAGGTCTCAA-3'.

Western blot

Cellular samples were gathered from every group and subjected to lysis using radioimmunoprecipitation assay (RIPA) lysis buffer (M052447, Mreda, Beijing, China) to extract the total protein. The concentration of extracted protein samples was determined using the Bradford Protein Assay Kit (G3522, GBCBIO, Guangzhou, China). 40 µg protein of each sample was segregated using 10% sodium dodecyl sulphate-polyacrylamide gel electrophoresis (SDS-PAGE), and subsequently, the proteins were transferred onto a polyvinylidene fluoride (PVDF) membrane. Afterward, the membrane was obstructed using phosphate buffered saline-tween (PBST) solution supplemented with 5% skim milk at room temperature for a duration of 2 hours. Then rabbit anti-rat Ghrelin (1:1000, orb11180, Biorbyt, Cambridge, UK), NLRP3 (1:1000, ET1610-93, HUABIO, Woburn, MA, USA), Caspase-1 (1:1000, ET1608-69, HUABIO, Woburn, MA, USA), and β-actin (1:1000, ET1702, HUABIO, Woburn, MA, USA) were added respectively and incubated at 4°C overnight. The membrane underwent three rounds of washing with TBST for 10 minutes each, followed by incubation with HRP-labeled goat anti-rabbit IgG (1:1000, A120-101P, Bethyl, Taibei, Taiwan, China) at room temperature for 2 h. Then the membrane was washed with TBST for 3 times, 5 min each time. A freshly prepared solution of enhanced chemiluminescence (A:B = 1:1) was applied to the side of the membrane containing the proteins. Subsequently, the membrane was exposed within a dark room. The duration of exposure was adapted in accordance with the luminous intensity to enable the development and fixation of the films. The results were analyzed with the Image J software processing system.

MTT

Cell samples from each group were seeded into a 96-well plate, 2×10³ cells per well, and cultured for 24 h. Then 10 µl (5 mg/mL) MTT (21795, Cayman) was added into each well and cultured the cells for another 4 h. The media of each well was carefully aspirated, and 150 µl dimethyl sulfoxide (DMSO) was introduced. The plate was vortexed for 10 min. The absorption (A) of each well at 490 nm wave length was determined to calculate the cell survival rate of each group. Cell viability (%) = (A_{experiment} -

$$\frac{A_{\text{blank}}}{(A_{\text{control}} - A_{\text{blank}})} \times 100.$$

Flow cytometry

To analyze the cell cycle, cells were cultured for a duration of 24 hours subsequent to the treatment, and then collected, washed with ice-cold germ-free PBS twice, and pelleted down by centrifugation at 1000 rpm for 6 min. Then -20°C pre-cooled 70% ethanol was added and the cells were fixed at 4°C for 12 h. Cells were centrifuged at 1500 rpm for 5min, washed with $1\times$ PBS, and resuspended in 400 μl propidium iodide (PI)/RNase staining buffer (BD Pharmingen, San Diego, CA, USA). Cells were applied to flow cytometer after being stained at 4°C in dark for 30 min. For detection of cell apoptosis, cells were cultured for 24 h after treatment, collected, and washed with ice-cold germ-free PBS twice. A total amount of 1×10^6 cells of each sample were pelleted down and resuspended with 250 μl $1\times$ binding buffer. Then 5 μl FITC labelled Annexin-V was added into 195 μl cell suspension, mixed gently, and let stand for 3 min. Then 10 μl 20 $\mu\text{g}/\text{ml}$ PI was added and mixed with each sample, and then incubated at room temperature in a dark environment for a span of 10 minutes. Finally, 400 μl $1\times$ binding buffer was added and mixed gently with the suspension, and the suspension was applied to flow cytometer (Gallios, Beckman Coulter. Inc, Brea, CA, USA).

Immunofluorescence

Coverslips were placed in 6-well plate in advance of transfection. After the H/R model has been established, cell-crewed coverslips were washed with PBS for 3 times, 5min each. The cells were fixed using a solution of 4% paraformaldehyde, followed by three subsequent washes with PBS. Extra PBS was blotted with blotting paper. The slides were blocked with goat serum at room temperature for 30 min. Then rabbit anti rat NLRP3 (1:200, ET-1610-93, HUABIO, Woburn, MA, USA), Caspase-1 (1:200, orb318090, Biorbyt, Cambridge, UK), p-AMPK (1:800, orb167533, Biorbyt, Cambridge, UK), AMPK (1:800, orb14583, Biorbyt, Cambridge, UK), p-MTOR (1:1000, orb501321, Biorbyt, Cambridge, UK), mTOR (1:1000, orb333935, Biorbyt, Cambridge, UK), β -actin (1:500, orb181785, Biorbyt, Cambridge, UK) polyclonal antibodies were added respectively, and incubated at 4°C overnight and at room temperature for another 60 min. The slides underwent four rounds of washing with PBS, after which they were exposed to incubation with FITC-labeled goat anti-rabbit IgG (1:500, Sgml102, Mlbio) in the dark for 1h. Then the slides were underwent three washes with PBS, 5min each, and counterstained with DAPI. Slides were sealed after adding antifade mounting medium, and then observed under fluorescent microscope (BK6000, Chongqing, China).

Statistical analysis

Statistic Package for Social Science (SPSS) 17.0 statistical analysis software (SPSS Inc., Chicago, IL, USA) was adopted for data processing. All experiments were repeated 3 times. The outcomes were shown in graphical format of $\bar{X}\pm\text{SD}$. One-way analysis of variance (ANOVA) was employed to analyze data among multi groups. Dunnett test was used for subsequent analysis, statistical significance was indicated with $P<0.05$.

Results

The expression pattern of ghrelin in each group

As shown in Figure 1A, cells in the H and H/R group expressed significantly fewer ghrelin mRNA than control ($P<0.05$). The mRNA levels of ghrelin were found to be even lower in the cells of the H/R groups as compared to those in the H group ($P<0.01$). As shown in Figure 1B, western blot results revealed that when compared with control, the protein level of ghrelin exhibited a noteworthy reduction ($P<0.05$), which was further decreased in H/R group ($P<0.01$). The protein level of NLRP3 showed a contrary trend compared with the ghrelin expression. In contrast to the control group, there was a distinct elevation in the expression of NLRP3 observed in both the H and H/R groups ($P<0.01$).

The role of ghrelin in the cell viability, cell cycle, and cell apoptosis of H/R treated H9C2 cells

As revealed by RT-PCR and western blot results displayed in Figure 2A and Figure 2B, respectively, in comparison to the H/R group, cells in ghrelin group expressed significantly higher amounts of ghrelin in both transcriptional and translational levels ($P<0.01$). As the results of the MTT assay (Figure 2C) and flow cytometry (Figure 3A, 3B), in comparison to the control, cells in the H/R group had lower cell viability, a larger proportion of cells in the G0/G1 phase, and higher apoptosis rate ($P<0.01$). Cells overexpressing ghrelin exhibited significantly higher cell viability, increased S phase, and less apoptosis ($P<0.05$).

The influence of ghrelin on both NLRP3 and caspase-1 expressions in H/R H9C2 cells

As shown in Figure 4A, positive signals of both NLRP3 and caspase-1 are located in the cytosol. The protein quantities of NLRP3 and caspase-1 were markedly elevated in cells subjected to H/R treatment, in comparison to the control ($P<0.01$), while overexpression of ghrelin was capable of reducing NLRP3 and caspase-1 expression induced by H/R ($P<0.01$). Besides the results of immunofluorescence (Figure 4A), the protein expression patterns of NLRP3 and caspase-1 were also validated by western

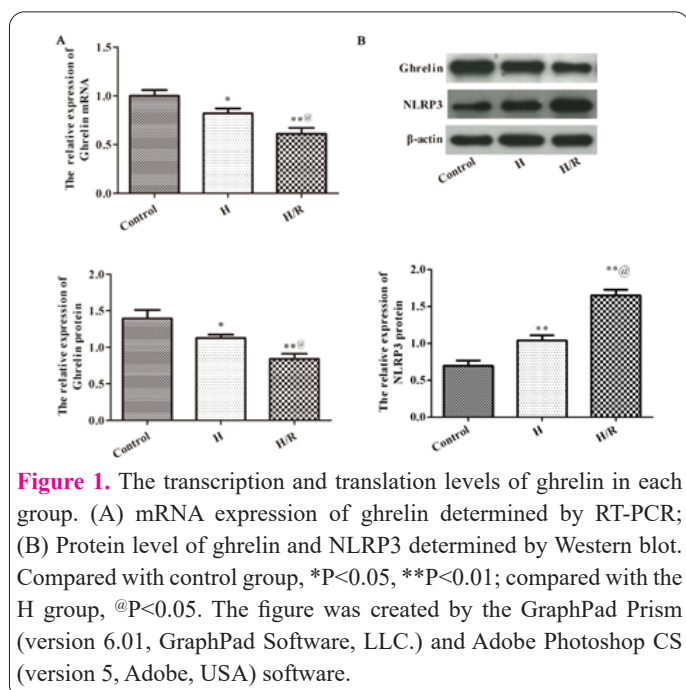
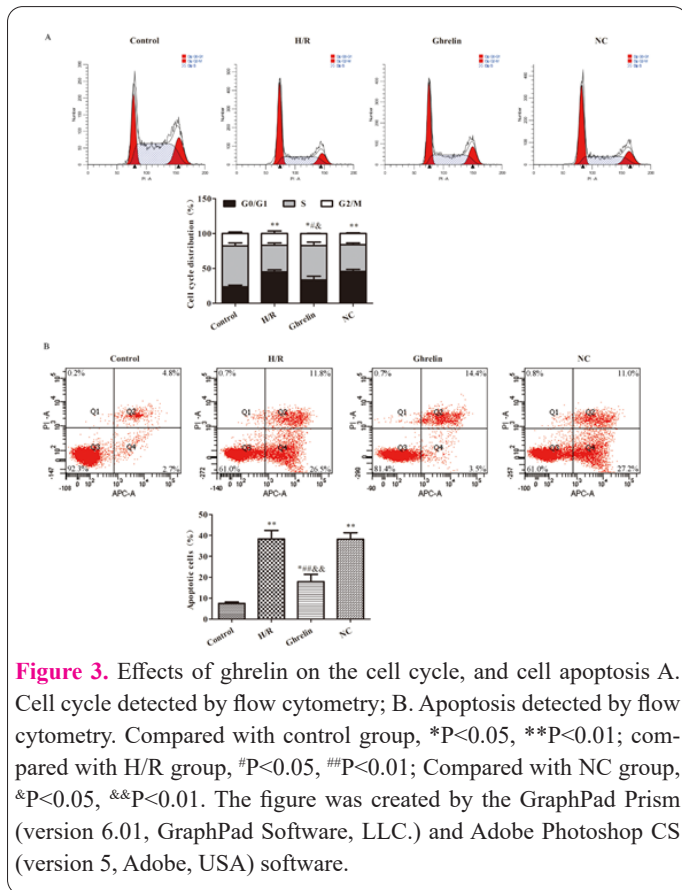
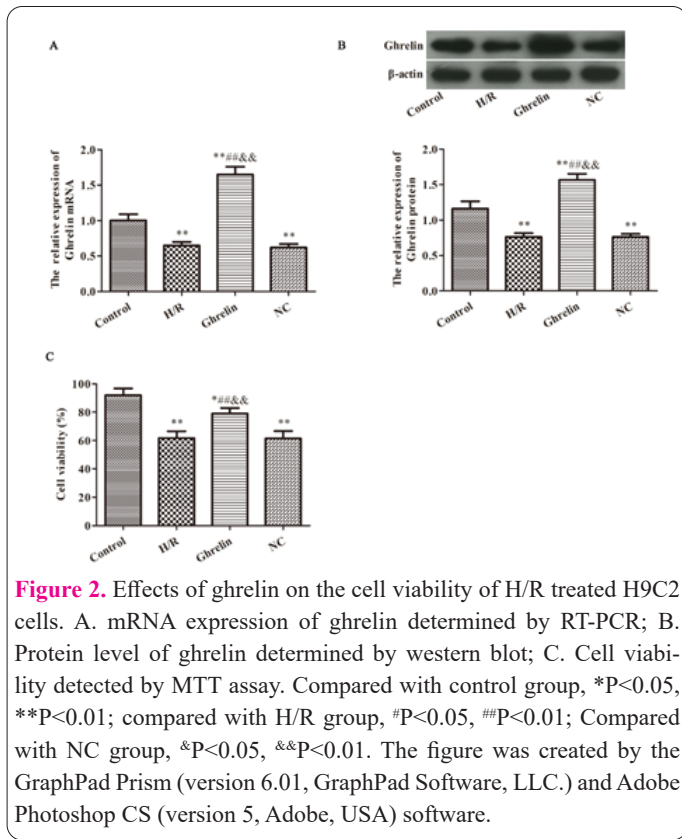


Figure 1. The transcription and translation levels of ghrelin in each group. (A) mRNA expression of ghrelin determined by RT-PCR; (B) Protein level of ghrelin and NLRP3 determined by Western blot. Compared with control group, $*P<0.05$, $**P<0.01$; compared with the H group, $@P<0.05$. The figure was created by the GraphPad Prism (version 6.01, GraphPad Software, LLC.) and Adobe Photoshop CS (version 5, Adobe, USA) software.



blot (Figure 4B), and the results were similar to the immunofluorescence experiments.

Effects of ghrelin and NLRP3 on cell viability, cell cycle, and apoptotic processes within H/R-treated H9C2 cells

Cells subjected to H/R treatment displayed notably elevated NLRP3 expression in comparison to control cells, as evidenced by both RT-PCR and Western blot analyses

(Figure 5A, B, $P < 0.05$). And the increase of NLRP3 could be diminished by overexpressing ghrelin ($P < 0.05$). In comparison to the ghrelin group, cells in the ghrelin +NLRP3 group had remarkably lower levels of NLRP3 mRNA ($P < 0.05$). As shown in 5C, Figure 6A and Figure 6B, ghrelin group cells had higher cell viability, decreased G0/G1 phase cell number, increased S phase cell number, and significantly reduced apoptosis ($P < 0.05$) in comparison to the NLRP3 group. In contrast to the ghrelin group,

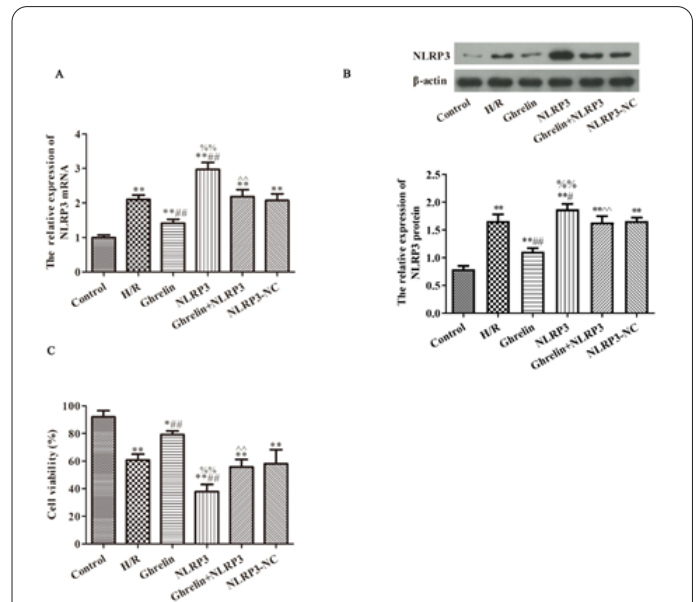
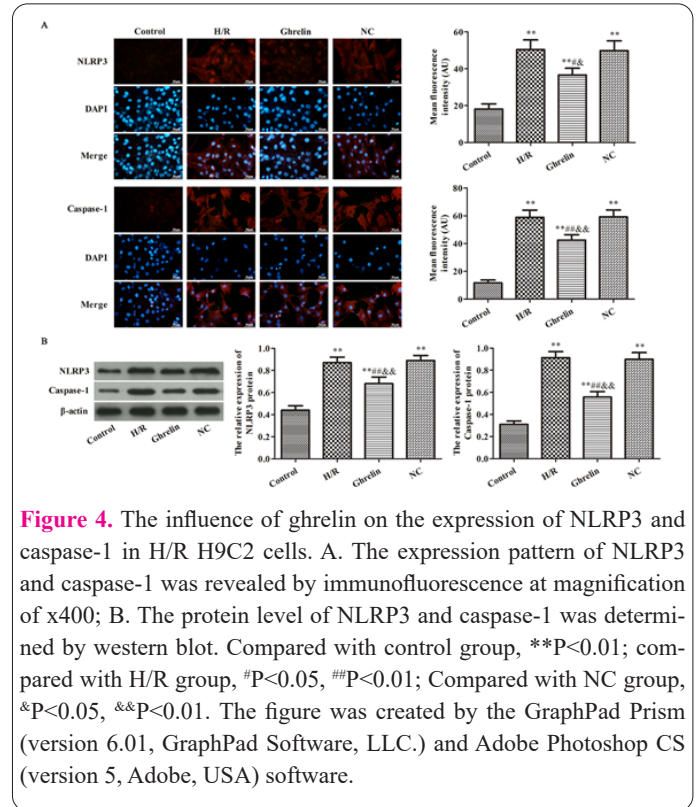


Figure 5. Effects of ghrelin together with NLRP3 on the cell viability of H/R treated H9C2 cells. A. NLRP3 mRNA expression determined by RT-PCR; B. Protein level of ghrelin in cells determined by western blot; C. Cell viability detected by MTT; Compared with control group, * $P < 0.05$, ** $P < 0.01$; compared with H/R group, # $P < 0.05$, ## $P < 0.01$; compared with Ghrelin group, % $P < 0.05$, %% $P < 0.01$; compared with NLRP3 group, ^ $P < 0.05$, ^^ $P < 0.01$. The figure was created by the GraphPad Prism (version 6.01, GraphPad Software, LLC.) and Adobe Photoshop CS (version 5, Adobe, USA) software.

cells in the ghrelin +NLRP3 group exhibited lower viability, higher G0/G1 phase versus S phase cell ratio, and larger proportion of apoptosis (P<0.05).

The influence of ghrelin together with NLRP3 on both NLRP3 and Caspase-1 expressions in H/R treated H9C2 cells

As depicted in Figure 7A, the expression patterns of NLRP3 and caspase-1 were analyzed by immunofluorescence. Compared with the H/R group, protein levels of NLRP3 and caspase-1 in ghrelin group cells exhibited a notable decrease (P<0.01). In addition, the NLRP3 and caspase-1 expression was increased in comparison to the H/R group (P<0.01). However, the protein quantities of NLRP3 and caspase-1 within the Ghrelin +NLRP3 group were markedly elevated in comparison to the ghrelin-only group (P<0.01). Similar findings were acquired through

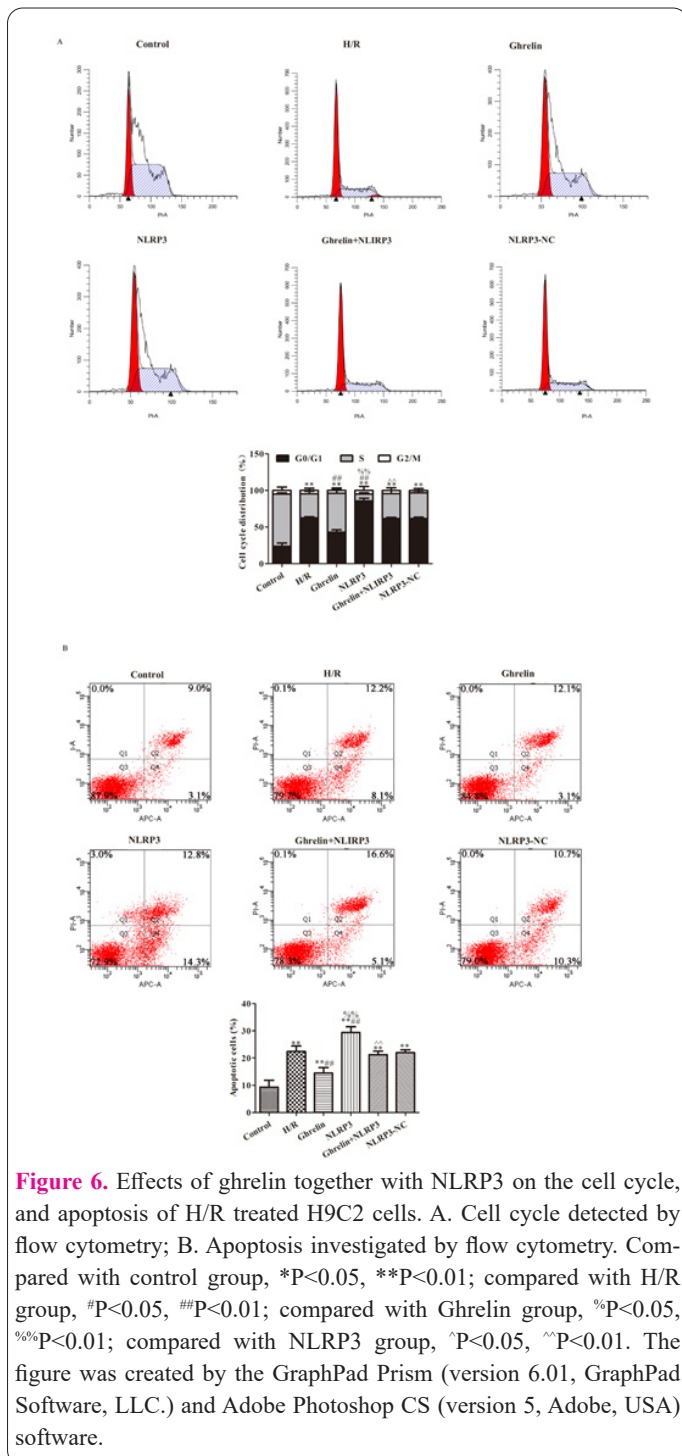


Figure 6. Effects of ghrelin together with NLRP3 on the cell cycle, and apoptosis of H/R treated H9C2 cells. A. Cell cycle detected by flow cytometry; B. Apoptosis investigated by flow cytometry. Compared with control group, *P<0.05, **P<0.01; compared with H/R group, #P<0.05, ###P<0.01; compared with Ghrelin group, %P<0.05, %%P<0.01; compared with NLRP3 group, ^P<0.05, ^^P<0.01. The figure was created by the GraphPad Prism (version 6.01, GraphPad Software, LLC.) and Adobe Photoshop CS (version 5, Adobe, USA) software.

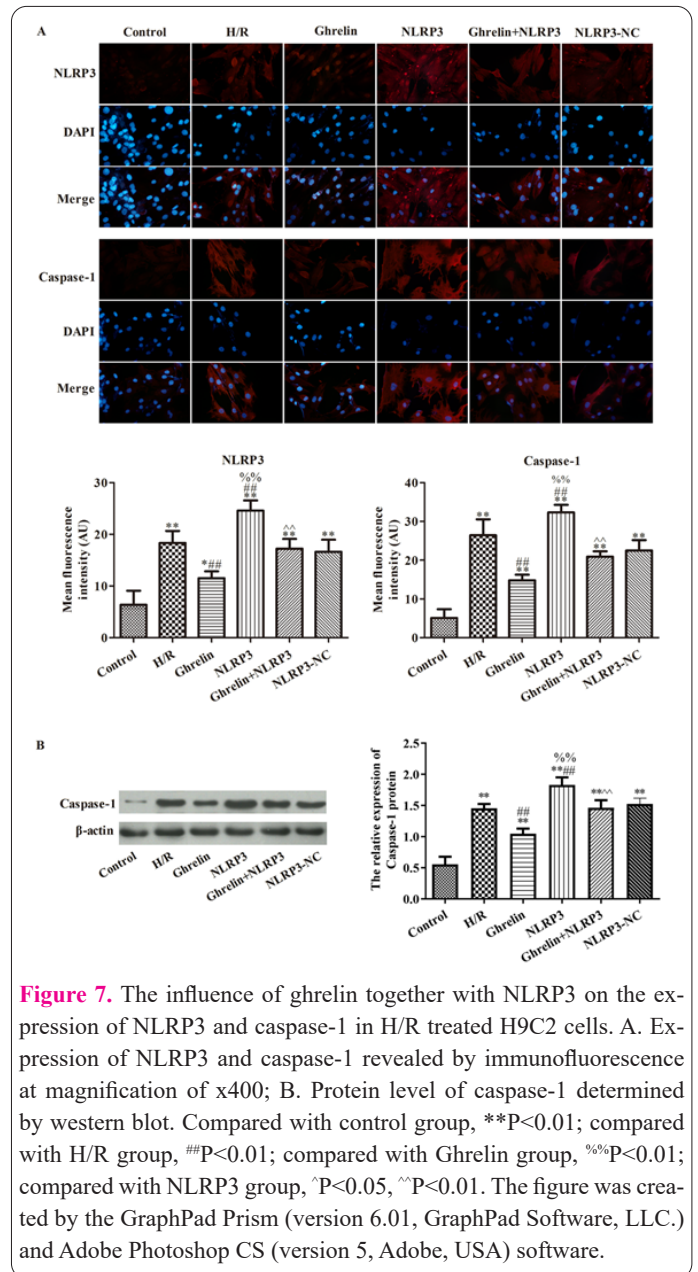


Figure 7. The influence of ghrelin together with NLRP3 on the expression of NLRP3 and caspase-1 in H/R treated H9C2 cells. A. Expression of NLRP3 and caspase-1 revealed by immunofluorescence at magnification of x400; B. Protein level of caspase-1 determined by western blot. Compared with control group, **P<0.01; compared with H/R group, ###P<0.01; compared with Ghrelin group, %%P<0.01; compared with NLRP3 group, ^P<0.05, ^^P<0.01. The figure was created by the GraphPad Prism (version 6.01, GraphPad Software, LLC.) and Adobe Photoshop CS (version 5, Adobe, USA) software.

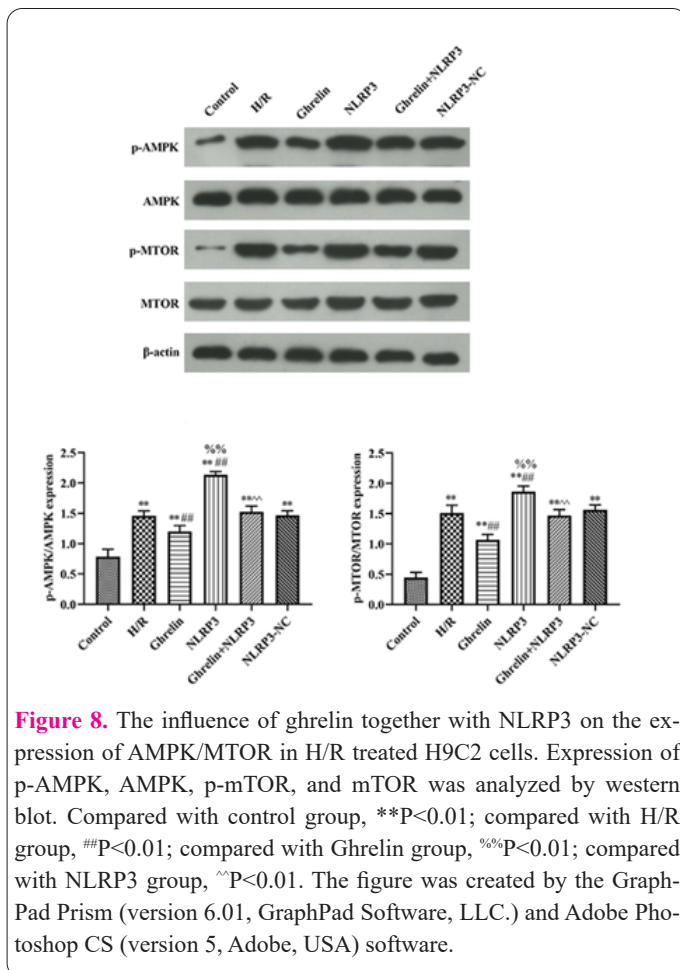
Western blot, as illustrated in Figure 7B.

The influence of ghrelin together with NLRP3 on the AMPK/mTOR Expression within H/R treated H9C2 cells

Western blot analysis was utilized to measure the expression levels of p-AMPK/AMPK and p-mTOR/mTOR within each respective group (Figure 8). Following H/R treatment, a notable increase in the phosphorylation of AMPK and mTOR was observed. However, this elevation in phosphorylation was mitigated by the overexpression of ghrelin (P<0.01). We also found that overexpression of NLRP3 notably increased the expression of p-AMPK/AMPK, p-mTOR/mTOR compared to the H/R group (P<0.01), and overexpression of NLRP3 concealed the roles of ghrelin.

Discussion

According to previous studies (24, 25), the H/R model was successfully established in H9C2 cells to investigate whether ghrelin is involved in H/R-induced pyroptosis. Ghrelin, a ligand for the growth hormone secretagogue



receptor, is produced within the submucosal layer of the stomach and subsequently released into the bloodstream. Ghrelin has been proven to be involved in cardiovascular diseases, including chronic heart failure, and myocardial infarction (15). In animal models, ghrelin administration promoted remodeling post-myocardial infarction, reduced the occurrence of fatal arrhythmias and prevented cardiac cell apoptosis (16-18). The related mechanisms included Raf-MEK1/2-ERK1/2 pathway (18), JAK2/STAT3 pathway (26) and Nrf2-NADPH-ROS pathway (27), etc. Nonetheless, the precise mechanisms through which ghrelin exerts its influences on the cardiovascular system remain incompletely understood.

Pyroptosis has been participated in the apoptosis of cardiomyocytes (28-30). Pyroptosis is a form of inflammatory-mediated cell death, which holds significant relevance in various pathological processes. In cells, the formation of NLRP3 inflammation could lead to pyroptosis. The NLRP3 inflammation, belonging to the inflammasome family, induces the NOD-like receptor NLRP3, the adaptor ASC and the effector enzyme caspase-1 (11). Activated caspase-1 triggers downstream expression of proinflammatory cytokines from pyroptotic dead cells. The relationship between ghrelin and NLRP3 inflammasome has been already revealed in multiple diseases, including renal fibrosis (31), brain injury (32), acute lung injury (33), and myocardial ischemia/reperfusion injury (20). According to previous reports, we obtained that ghrelin could inhibit the NLRP3 pathway to alleviate multiple disease-induced injury.

In our study, the relationship between ghrelin and NLRP3 in H/R-induced H9C2 cells was investigated. It

was found that overexpression of ghrelin was capable of reducing the levels of NLRP3 and caspase-1, increasing the cell viability and reducing the cells apoptosis. Furthermore, the protective effects of ghrelin were covered by overexpressing NLRP3. These results indicated a negative correlation between ghrelin and NLRP3 in H/R-induced H9C2 cells. However, the above results were only confirmed in vitro, more in vivo experiments are needed to carry out.

In existing reports, ghrelin conferred protection to H9C2 cells against H/R induced cell death via PI3K/AKT and AMPK pathway (34, 35). NLRP3 activation could induce numerous inflammatory pathways, including NF- κ B, AMPK/mTOR, PI3K/Akt (28-30). In our study, we also found that ghrelin suppressed the phosphorylation of AMPK and mTOR in H/R-treated H9C2 cells, which was consistent with previous studies. Furthermore, we found that overexpression of NLRP3 masked the effects of ghrelin on the AMPK/mTOR pathway, suggesting that ghrelin inhibited the AMPK/mTOR pathway through suppressing the NLRP3 activation.

In conclusion, ghrelin could exert protective effects on H/R-treated H9C2 cells by suppressing pyroptosis via NLRP3. This finding might be helpful to find new target and develop new therapies of ischemia-reperfusion-induced myocardial infarction.

Funding

None declared.

Conflict of interest

The authors declare that they have no competing interests.

Acknowledgments

The authors thank all the participants involved in this study.

References

- Reiter RJ, Tan DX. Melatonin: a novel protective agent against oxidative injury of the ischemic/reperfused heart. *Cardiovasc Res* 2003; 58(1): 10-19.
- Dhalla NS, Temsah RM, Netticadan T. Role of oxidative stress in cardiovascular diseases. *J Hypertens* 2000; 18(6): 655-673.
- Piacentini L, Karliner JS. Altered gene expression during hypoxia and reoxygenation of the heart. *Pharmacol Therapeut* 1999; 83(1): 21-37.
- Dai D, Yang J, Zhao C, et al. Effect of Geranylgeranyl Pyrophosphate Synthase on Hypoxia/Reoxygenation-Induced Injury in Heart-Derived H9c2 Cells. *Int Heart J* 2018; 59(4): 821-828.
- Crawford RM, Jovanovic S, Budas GR, et al. Chronic mild hypoxia protects heart-derived H9c2 cells against acute hypoxia/reoxygenation by regulating expression of the SUR2A subunit of the ATP-sensitive K⁺ channel. *J Biol Chem* 2003; 278(33): 31444-31455.
- Zhang RY, Qiao ZY, Liu HJ, Ma JW. Sonic hedgehog signaling regulates hypoxia/reoxygenation-induced H9C2 myocardial cell apoptosis. *Exp Ther Med* 2018; 16(5): 4193-4200.
- Su G, Sun G, Liu H, Shu L, Zhang W, Liang Z. Prokineticin 2 relieves hypoxia/reoxygenation-induced injury through activation of Akt/mTOR pathway in H9c2 cardiomyocytes. *Artif Cell Nanomed B* 2020; 48(1): 345-352.
- Shi J, Gao W, Shao F. Pyroptosis: Gasdermin-Mediated Programmed Necrotic Cell Death. *Trends Biochem Sci* 2017; 42(4): 245-

- 254.
9. Wu J, Fernandes-Alnemri T, Alnemri ES. Involvement of the AIM2, NLRC4, and NLRP3 inflammasomes in caspase-1 activation by *Listeria monocytogenes*. *J Clin Immunol* 2010; 30(5): 693-702.
 10. Shi J, Zhao Y, Wang K, et al. Cleavage of GSDMD by inflammatory caspases determines pyroptotic cell death. *Nature* 2015; 526(7575): 660-665.
 11. Liu D, Zeng X, Li X, Mehta JL, Wang X. Role of NLRP3 inflammasome in the pathogenesis of cardiovascular diseases. *Basic Res Cardiol* 2018; 113(1): 5.
 12. Zhaolin Z, Guohua L, Shiyuan W, Zuo W. Role of pyroptosis in cardiovascular disease. *Cell Proliferat* 2019; 52(2): e12563.
 13. Toldo S, Abbate A. The NLRP3 inflammasome in acute myocardial infarction. *Nat Rev Cardiol* 2018; 15(4): 203-214.
 14. Lei Q, Yi T, Chen C. NF-kappaB-Gasdermin D (GSDMD) Axis Couples Oxidative Stress and NACHT, LRR and PYD Domains-Containing Protein 3 (NLRP3) Inflammasome-Mediated Cardiomyocyte Pyroptosis Following Myocardial Infarction. *Med Sci Monitor* 2018; 24(6044-6052).
 15. Tokudome T, Kangawa K. Physiological significance of ghrelin in the cardiovascular system. *P Jpn Acad B-Phys* 2019; 95(8): 459-467.
 16. Soeki T, Kishimoto I, Schwenke DO, et al. Ghrelin suppresses cardiac sympathetic activity and prevents early left ventricular remodeling in rats with myocardial infarction. *Am J Physiol-Heart C* 2008; 294(1): H426-H432.
 17. Schwenke DO, Tokudome T, Kishimoto I, et al. One dose of ghrelin prevents the acute and sustained increase in cardiac sympathetic tone after myocardial infarction. *Endocrinology* 2012; 153(5): 2436-2443.
 18. Eid RA, Alkhateeb MA, Al-Shraim M, et al. Ghrelin prevents cardiac cell apoptosis during cardiac remodelling post experimentally induced myocardial infarction in rats via activation of Raf-MEK1/2-ERK1/2 signalling. *Arch Physiol Biochem* 2019; 125(2): 93-103.
 19. Liu F, Li Z, He X, Yu H, Feng J. Ghrelin Attenuates Neuroinflammation and Demyelination in Experimental Autoimmune Encephalomyelitis Involving NLRP3 Inflammasome Signaling Pathway and Pyroptosis. *Front Pharmacol* 2019; 10(1320).
 20. Wang Q, Lin P, Li P, et al. Ghrelin protects the heart against ischemia/reperfusion injury via inhibition of TLR4/NLRP3 inflammasome pathway. *Life Sci* 2017; 186(50-58).
 21. Benoist L, Chadet S, Genet T, et al. Stimulation of P2Y11 receptor protects human cardiomyocytes against Hypoxia/Reoxygenation injury and involves PKCepsilon signaling pathway. *Sci Rep-Uk* 2019; 9(1): 11613.
 22. Feng X, Luo Q, Wang H, Zhang H, Chen F. MicroRNA-22 suppresses cell proliferation, migration and invasion in oral squamous cell carcinoma by targeting NLRP3. *J Cell Physiol* 2018; 233(9): 6705-6713.
 23. Castelblanco M, Lugin J, Ehrichtiou D, et al. Hydrogen sulfide inhibits NLRP3 inflammasome activation and reduces cytokine production both in vitro and in a mouse model of inflammation. *J Biol Chem* 2018; 293(7): 2546-2557.
 24. Sayed N, Tambe P, Kumar P, Jadhav S, Paknikar KM, Gajbhiye V. miRNA transfection via poly(amidoamine)-based delivery vector prevents hypoxia/reperfusion-induced cardiomyocyte apoptosis. *Nanomedicine-Uk* 2020; 15(2): 163-181.
 25. Vilar M, Murillo-Carretero M, Mira H, Magnusson K, Besset V, Ibanez CF. Bex1, a novel interactor of the p75 neurotrophin receptor, links neurotrophin signaling to the cell cycle. *Embo J* 2006; 25(6): 1219-1230.
 26. Eid RA, Alkhateeb MA, Eleawa S, et al. Cardioprotective effect of ghrelin against myocardial infarction-induced left ventricular injury via inhibition of SOCS3 and activation of JAK2/STAT3 signaling. *Basic Res Cardiol* 2018; 113(2): 13.
 27. Wang Q, Liu AD, Li TS, Tang Q, Wang XC, Chen XB. Ghrelin ameliorates cardiac fibrosis after myocardial infarction by regulating the Nrf2/NADPH/ROS pathway. *Peptides* 2021; 144(170613).
 28. Wang Q, Wei S, Zhou S, et al. Hyperglycemia aggravates acute liver injury by promoting liver-resident macrophage NLRP3 inflammasome activation via the inhibition of AMPK/mTOR-mediated autophagy induction. *Immunol Cell Biol* 2020; 98(1): 54-66.
 29. Shao A, Wu H, Hong Y, et al. Hydrogen-Rich Saline Attenuated Subarachnoid Hemorrhage-Induced Early Brain Injury in Rats by Suppressing Inflammatory Response: Possible Involvement of NF-kappaB Pathway and NLRP3 Inflammasome. *Mol Neurobiol* 2016; 53(5): 3462-3476.
 30. Wang K, Zhang Y, Cao Y, et al. Glycyrrhetic acid alleviates acute lung injury by PI3K/AKT suppressing macrophagic Nlrp3 inflammasome activation. *Biochem Bioph Res Co* 2020; 532(4): 555-562.
 31. Ling L, Yang M, Ding W, Gu Y. Ghrelin attenuates UUO-induced renal fibrosis via attenuation of Nlrp3 inflammasome and endoplasmic reticulum stress. *Am J Transl Res* 2019; 11(1): 131-141.
 32. Cheng Y, Chen B, Xie W, et al. Ghrelin attenuates secondary brain injury following intracerebral hemorrhage by inhibiting NLRP3 inflammasome activation and promoting Nrf2/ARE signaling pathway in mice. *Int Immunopharmacol* 2020; 79(106180).
 33. Shao XF, Li B, Shen J, et al. Ghrelin alleviates traumatic brain injury-induced acute lung injury through pyroptosis/NF-kappaB pathway. *Int Immunopharmacol* 2020; 79(106175).
 34. Chen Y, Wang H, Zhang Y, Wang Z, Liu S, Cui L. Pretreatment of ghrelin protects H9c2 cells against hypoxia/reoxygenation-induced cell death via PI3K/AKT and AMPK pathways. *Artif Cell Nanomed B* 2019; 47(1): 2179-2187.
 35. Baldanzi G, Filigheddu N, Cutrupi S, et al. Ghrelin and des-acyl ghrelin inhibit cell death in cardiomyocytes and endothelial cells through ERK1/2 and PI 3-kinase/AKT. *J Cell Biol* 2002; 159(6): 1029-1037.